Pergamon

Int. J. Heat Mass Transfer. Vol. 38, No. 2, pp. 363–369, 1995

0017–9310/95 $9.50 + 0.00

0017–9310(94)00160–X

The stability of a single-cell steady-state solution in a triangular enclosure

HAYDEE SALMUN†

Robert Hooke Institute, The Observatory, Clarendon Laboratory, Parks Road, Oxford OX1 3PU, U.K.

(*Received* 29 *January* 1993 *and in final form* 18 *March* 1994)

Abstract—For a triangular domain with a sloping cold upper surface and warm lower horizontal surface, and when the aspect ratio, or equivalently the slope, is very small, the three-dimensional problem may be reduced to a local two-dimensional problem between horizontally parallel planes at each location along the enclosure horizontal extent, reducing the problem to the classical Rayleigh–Bénard there. In this simple way it is possible to obtain a guide to the values of the critical Rayleigh number above which a known steady-state solution is not stable to perturbations in the flow in a specified geometry.

1. INTRODUCTION

Poulikakos and Bejan [1] developed a model for the circulation patterns in a two-dimensional triangular cavity, with cold upper wall and warm horizontal bottom wall. Using the techniques described in ref. [2], they were able to find analytical expressions for the steady state in the form of asymptotic series valid for infinitely shallow enclosures. This solution consisted of a single convective cell, which they found (numerically) to be stable over a wide range of the parameters that govern the behaviour of this system. More recent works using similar geometries, however, seem to indicate that with the higher values of the Rayleigh number used by ref. [1] the steady-state circulation in irregular enclosures is characterized by a multi-cell structure, typical of the Rayleigh–Bénard convection systems. In particular, Salmun [3] reports results from considering basically the same problem which show the break down of the single cell into a multi-cell structure as the global Rayleigh number that characterizes the enclosure is increased beyond a value of approximately 4×10^3. This result suggests that the single-cell steady-state solution to this problem is not stable to perturbations in the system as this parameter increases, and this fact motivated the present paper.

The occurrence of secondary flows, in the form of longitudinal rolls, superposed upon the natural convection main flow on inclined surfaces has been observed experimentally [4, 5] and analysed extensively [6]. In ref. [6] a brief review of this subject is also provided. This work, which considered rectangular enclosures, suggests that when the angle of inclination of the surface that is the source of instabilities is small (measured with respect to the horizontal) then the most unstable perturbation takes the form of longitudinal rolls with their axes aligned with the direction of the slope. This is the assumed form of the perturbation that will be considered in the present note.

The recent work of Farrow and Patterson [7] provides a method of analysing the stability of a basic flow solution in a wedge-shapped geometry that can be applied to the present problem in a straightforward manner. The main objective of the present contribution is to present the simple results obtained from a linear stability analysis of the steady-state asymptotic solution in a shallow triangular enclosure, and to show that it is not stable to the type of instabilities expected in fluid layers heated differentially along horizontal boundaries. In Section 2 the mathematical problem is described and the solutions obtained by ref. [1], which will constitute the basic state upon which a perturbation will be superimposed, briefly summarized. The stability analysis is detailed in Section 3, where the final simple results are discussed, and Section 4 summarizes the present work. Although the validity of these results are limited to the context of the linear theory, they are in a remarkable good agreement with the detailed numerical results reported in ref. [3] and, in turn, lend further support to those results.

2. PROBLEM FORMULATION

The non-dimensional Navier–Stokes equations that describe the motion in the three-dimensional wedge-like geometry, whose cross-section in the plane (x, y) is depicted in Fig. 1, are:

$$\frac{\partial u}{\partial t} + A^2 Ra\left(u\frac{\partial u}{\partial x} + v\frac{\partial u}{\partial y}\right) + Ra\, w\frac{\partial u}{\partial z} = -Pr\frac{\partial p}{\partial x} + Pr\,\nabla_A^2 u, \quad (1)$$

† Present address: Department of Geography and Environmental Engineering, The Johns Hopkins University, Baltimore, MD 21218-2686, U.S.A.

NOMENCLATURE

A	aspect ratio, H/L
Gr	Grashof number, $g\alpha(T_h - T_l)H^3/\nu^2$
g	acceleration due to gravity
H	enclosure maximum height
i	$\sqrt{-1}$
$\mathcal{J}$	Jacobian operator: for any given functions A and B, $\mathcal{J}(A,B) = (\partial A/\partial x)(\partial B/\partial y) - (\partial B/\partial x)(\partial A/\partial y)$
L	enclosure horizontal extent
m	wave number
m_{crit}	critical wave number
∇_A^2	non-dimensional Laplacian operator: $\nabla_A^2 = A^2(\partial^2/\partial x^2) + (\partial^2/\partial y^2) + (\partial^2/\partial z^2)$
Pr	Prandtl number, ν/κ
p	pressure
P	perturbation pressure
Ra, Ra_H	global Rayleigh number, $g\alpha(T_h - T_l)H^3/\nu\kappa = Gr \times Pr$
Ra_x	local Rayleigh number, Ra_H/x
Ra_{crit}	critical Rayleigh number
t	time
T	temperature
T_h	temperature of the warm horizontal wall
T_l	reference temperature, that of the cold sloping wall
$\mathbf{u}$	velocity vector
$\mathbf{U}$	perturbation velocity vector
u, v, w	velocity components
V, W	perturbation velocity components
x, y, z	Cartesian coordinates system, y vertical.

Greek symbols

α	coefficient of thermal expansion
ε	perturbation parameter
η	wave number
θ, Θ	perturbation temperature
κ	thermal conductivity
ν	kinematic viscosity
σ	growth rate of perturbation
ϕ, Ψ	perturbation stream function
ψ	two-dimensional stream function
ω_x	x-component of the perturbation vorticity field.

Subscript

s	characteristic scales.

Superscript

0	zeroth order solutions $[O(A^0)]$ and basic state flow.

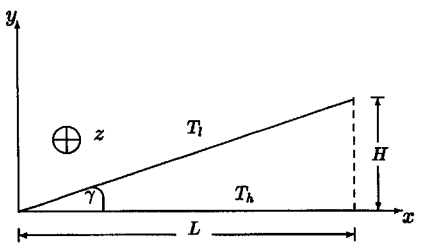

Fig. 1. A cross-section of a three-dimensional wedge-like geometry. The z-coordinate is perpendicular to the (x, y) plane of the figure and positive out of the page.

$$A^2\frac{\partial v}{\partial t} + A^4 Ra\left(u\frac{\partial v}{\partial x} + v\frac{\partial v}{\partial y}\right) + A^2 Ra\, w\frac{\partial v}{\partial z} = -Pr\frac{\partial p}{\partial y} + A^2 Pr\,\nabla_A^2 v + Pr\,T, \quad (2)$$

$$\frac{\partial w}{\partial t} + A^2 Ra\left(u\frac{\partial w}{\partial x} + v\frac{\partial w}{\partial y}\right) + Ra\, w\frac{\partial w}{\partial z} = -Pr\frac{\partial p}{\partial z} + Pr\,\nabla_A^2 w, \quad (3)$$

$$\frac{\partial T}{\partial t} + A^2 Ra\left(u\frac{\partial T}{\partial x} + v\frac{\partial T}{\partial y}\right) + Ra\, w\frac{\partial T}{\partial z} = \nabla_A^2 T, \quad (4)$$

$$A^2\left(\frac{\partial u}{\partial x} + \frac{\partial v}{\partial y}\right) + \frac{\partial w}{\partial z} = 0, \quad (5)$$

where ∇_A^2 is the non-dimensional Laplacian operator defined in the Nomenclature. The z-coordinate is perpendicular to the plane of the figure and positive in the direction towards the reader. The system is subject to the boundary conditions:

$$u = v = w = 0 \quad T = 1 \quad \text{on} \quad y = 0, \quad (6)$$

$$u = v = w = 0 \quad T = 0 \quad \text{on} \quad y = x, \quad (7)$$

and to the initial conditions $u = v = w = 0$, $T = 1$ at $t = 0$.

The scales used in the non-dimensionalization scheme are derived from considering the appropriate balance of forces valid for laminar flow in fluids of $Pr \approx O(1)$, namely: buoyancy forces are mainly balanced by viscous forces. The length, velocity and time-scales are:

$$x_s = L \quad y_s = H \quad z_s = H$$

$$u_s = A\,Gr\left(\frac{\nu}{H}\right) \quad v_s = A^2\,Gr\left(\frac{\nu}{H}\right)$$

$$w_s = Gr\frac{\nu}{H} \quad t_s = \frac{H^2}{\kappa},$$

respectively. The non-dimensional temperature field is measured relative to the temperature of the sloping wall and contains $T_s = \Delta T = T_h - T_l$ as the temperature scale. It should be noted that the Grashof number, Gr, is based on the enclosure height, the

maximum separation distance between the two intersecting boundaries, which is considered constant. The vertical pressure gradient, readily estimated from the y-momentum equation, is $\approx g\alpha\Delta T$ while the horizontal pressure gradient term is $\approx Ag\alpha\Delta T$. The pressure gradient term in the z-direction is also $\approx g\alpha\Delta T$.

If $w = 0$ and variations in the z-direction are neglected, then the system of equations that results describes the two-dimensional problem studied in ref. [1]. The usual elimination of the pressure terms and use of the stream function in two dimensions yields the non-dimensional equations, which for the steady-state flow are:

$$Ra\,A^2\mathscr{J}\left(A^2\frac{\partial^2\psi}{\partial x^2}+\frac{\partial^2\psi}{\partial y^2},\psi\right)$$

$$=Pr\left(A^2\frac{\partial^2}{\partial x^2}+\frac{\partial^2}{\partial y^2}\right)\left(A^2\frac{\partial^2\psi}{\partial x^2}+\frac{\partial^2\psi}{\partial y^2}\right)-\frac{\partial T}{\partial x},$$

$$Ra\,A^2\mathscr{J}(T,\psi)=\left(A^2\frac{\partial^2}{\partial x^2}+\frac{\partial^2}{\partial y^2}\right)T, \qquad (8)$$

where the Jacobian operator $\mathscr{J}$ is defined as usual (see Nomenclature).

Details of the method of solution and the solutions themselves may be found in ref. [1], and are briefly summarized below. In the limit $A \to 0$, solutions for $\psi(x,y)$ and $T(x,y)$ in the form of an asymptotic series in A^2 can be found, which satisfy the boundary conditions:

$$T=1 \quad \psi=0 \quad \frac{\partial\psi}{\partial y}=0 \quad \text{on} \quad y=0,$$

$$T=0 \quad \psi=0 \quad \frac{\partial\psi}{\partial y}=0 \quad \text{on} \quad y=f(x), \qquad (9)$$

where $f(x)$ describes the shape of the upper wall. In the simple case of a shallow enclosure with a flat top boundary, $f(x) = x$ and the solution to lowest order (the largest contribution to the asymptotic series in any case) which is of interest here is given by:

$$T^0=1-\frac{y}{x},$$

$$\psi^0=\frac{1}{Pr}\left(\frac{1}{120}\frac{y^5}{x^2}-\frac{1}{40}y^3+\frac{1}{60}xy^2\right). \qquad (10)$$

This solution represents slightly tilted and evenly separated isotherms which give rise to a steady counterclockwise convective cell that fills in the entire domain. At any given x the longitudinal flow in the cavity is of the shear-type. In this approximation, the end-turn region in the neighbourhood of $x = 1$, infinitely short, serves to turn the flow by 180° and has no other effect on the circulation or heat transfer in the enclosure. The isotherm patterns in the limit $A \to 0$ are consistent with a system in which the mechanism that dominates the heat transfer across the cavity is conduction.

3. STABILITY ANALYSIS

To examine the stability of the zeroth-order steady-state solution to small perturbations in the flow and to determine a critical Rayleigh number above which secondary motion associated with instabilities may be expected, the approach used in ref. [7] is followed. Consider the $O(A^0)$ flow given by equation (10) and let this initial state be slightly perturbed according to the following expressions:

$$(\mathbf{u}, T, p) = (\mathbf{u}^0+\varepsilon\mathbf{U}, T^0+\varepsilon\Theta, p+\varepsilon P), \qquad (11)$$

where $\varepsilon \ll 1$ is the perturbation parameter, $\mathbf{u}^0 = (u^0, v^0)$ and $\mathbf{U} = (0, V/A^2, W)$; the factor $(1/A^2)$ is introduced here so that V and W are of the same order (cf. velocity scales). Alternatively, the perturbation stream function in the (y,z) plane considered below can be defined including that factor to achieve the same end. Since only longitudinal modes of perturbation are considered, the perturbation fields are x-independent, although, as seen below, the set of equations that describes the perturbed system depends on x. To obtain the linearized equations of motion that govern the perturbed state, substitute the perturbation functions into equations (1)–(5) and linearize the result with respect to ε. Note that $O(A^2, A^4)$ terms are negligibly small, since the condition $A \to 0$ holds. The $O(\varepsilon)$ equations that result are:

$$Ra\,V\frac{\partial u^0}{\partial y}=-Pr\frac{\partial P}{\partial x}, \qquad (12)$$

$$\frac{\partial V}{\partial t}=-Pr\frac{\partial P}{\partial y}+Pr\,\nabla^2 V+Pr\,\Theta, \qquad (13)$$

$$\frac{\partial W}{\partial t}=-Pr\frac{\partial P}{\partial z}+Pr\,\nabla^2 W, \qquad (14)$$

$$\frac{\partial\Theta}{\partial t}+Ra\,V\frac{\partial T^0}{\partial y}=\nabla^2\Theta, \qquad (15)$$

$$\frac{\partial V}{\partial y}+\frac{\partial W}{\partial z}=0, \qquad (16)$$

where here $\nabla^2 = \partial^2/\partial y^2+\partial^2/\partial z^2$ only.

It is immediately evident that the basic state flow u^0 is not involved directly in the mean balances of the secondary motion, implying that within the approximations considered here the stability of the flow does not depend explicitly on u^0. Consequently, the three-dimensional stability problem can be reduced to a two-dimensional problem for an infinitely long wedge-like geometry. Consider the perturbation vorticity component in the x-direction,

$$\omega_x=\frac{\partial W}{\partial y}-\frac{\partial V}{\partial z},$$

and use equation (16) to introduce a perturbation stream function Ψ so that $\omega_x = -\nabla^2\Psi$. In terms of the perturbation fields, Ψ and Θ, the system of equations above may be reduced to:

$$\frac{\partial}{\partial t}\nabla^2\Psi = Pr\nabla^4\Psi + \frac{\partial\Theta}{\partial z}, \tag{17}$$

$$\frac{\partial\Theta}{\partial t} + Ra\frac{\partial\Psi}{\partial z}\frac{\partial T^0}{\partial y} = \nabla^2\Theta, \tag{18}$$

with boundary conditions:

$$\Psi = \frac{\partial\Psi}{\partial y} = 0 \quad \Theta = 0 \quad \text{on} \quad y = 0, x. \tag{19}$$

The explicit dependence of the (y, z) perturbation equations on x, through the boundary conditions, expresses the locality of this problem now; at every location x, solutions to equations (17)–(19) will be sought and the instability will be determined by local conditions.

Perturbation quantities are described by the set of normal modes:

$$(\Psi, \Theta) = [\phi(y), \theta(y)] \times e^{imz+\sigma t}, \tag{20}$$

where m is the wave number of the disturbance and σ is a constant (both real). The real part of functions is implicitly understood in this section. Substituting equation (20) into (17) and (18), and eliminating θ from the equations that result, yields a single equation in ϕ:

$$\left(D^2 - m^2 - \frac{\sigma}{Pr}\right)(D^2 - m^2 - \sigma)(D^2 - m^2)\phi = m^2\, Ra\, DT^0\phi, \tag{21}$$

where $D = \mathrm{d}/\mathrm{d}y$. The transition from stability to instability occurring via a stationary state (see ref. [8] for a discussion on the classical Rayleigh–Bénard problem) will be described by equation (21) when $\sigma = 0$.

At this point it is useful to recall that the Rayleigh number is a non-dimensional parameter defined in terms of fluid properties (ν, κ, etc.) and the destabilizing temperature gradient of the basic state. In the present system, the dimensional basic state temperature is given by [cf. equation (10)] $T^0_{\mathrm{dim}} = (1-(y/x))\Delta T + T_1$ so that its vertical gradient is:

$$\left|\frac{1}{H}\frac{\partial}{\partial y}T^0_{\mathrm{dim}}\right| = \frac{\Delta T}{Hx},$$

and defines:

$$Ra_x = \frac{g\alpha\Delta T H^3}{\nu\kappa}\frac{1}{x},$$

where x is non-dimensional. Let now $Ra_x = Ra_H/x$, where Ra_H stresses that the Rayleigh number as defined previously is based on the original enclosure height, a constant taken as the characteristic vertical length-scale. This expression may be thought of as the relation between global and local Rayleigh numbers and it anticipates that, within the context of this analysis, there is not a single value of Ra below which the basic flow solution considered here will be stable, since $0 < Ra_x < \infty$ as x decreases towards zero, respectively. This analysis may, however, provide for a lower bound on the values of Ra that can be allowed if instabilities in the flow are to be prevented, as will be seen below.

The marginal state is then described by:

$$(D^2 - m^2)^3\phi = -m^2\, Ra_x\phi, \tag{22}$$

where $DT^0 = -(1/x)$ from equation (10) has been used. The solutions to equation (22) must satisfy the boundary conditions:

$$\phi = D\phi = (D^2 - m^2)^2\phi = 0 \quad \text{on} \quad y = \pm\tfrac{1}{2}x. \tag{23}$$

In writing equation (23) the symmetry of this problem with respect to the two bounding surfaces was used. This is: the origin of y was translated to lie midway between the two intersecting surfaces, along an axis that bisects the wedge, so that the fluid is assumed to be confined between $y = \pm\frac{1}{2}x$ rather than between $y = 0, x$. Although strictly speaking, the fluid is now confined between $y = \pm[\frac{1}{2}x + O(A^2)]$, for this is the equation of the bisecting line, for the present case ($A \to 0$) the assumption is amply justified. Equations (22) and (23) express the classical characteristic value problem for Ra_x: only for some values of Ra_x, for given m, will this sixth-order differential equation allow for non-trivial solutions. Moreover, in this case, this condition must be satisfied at a given location x. Then the critical value of Ra_x at which the instability may first occur, Ra_{crit}, is the smallest positive value of Ra_x for a given m and may be thought of as parametrically dependent on the variable x. The disturbances present at marginal stability are characterized by wave numbers denoted by m_{crit}.

In summary the problem now has been transformed as follows: at each location x along the wedge, the classical instability problem of two rigid parallel plates, vertically separated by a distance $\pm\frac{1}{2}x$ and kept at different temperatures, is solved. In the classical case, that of horizontal boundaries, equations (22) and (23) describe the behaviour that must be satisfied by the vertical structure of the (three-dimensional) velocity perturbation field (all the velocity field, in fact, since in that case the basic state is that of rest and purely conductive). In the present case, and within the validity of the small slope approximation, the problem to $O(A^0)$ can be cast in terms of the two-dimensional [in the (y, z) plane] stream function perturbation field with a basic state represented by a very slow convective cell which results in a quasi-conductive steady-state temperature field. Mathematically, however, the problems are identical, hence the method of solution for $\phi(y)$ here is the same as that for $w(y)$ in the classical Bénard problem, details of which can be found in ref. [8] (Chap. II) and is briefly summarised here. The only difference, as mentioned earlier, is the parametric dependence on x, which is now included above in the definition of Ra_x and hence the implications for the stability of the

basic flow will be different, but in essence the present problem is now solved.

The evenness of the operator in equation (22) and the symmetry in boundary conditions (23) imply that the solutions to equation (22) will separate into even and odd solutions, the lowest mode being an even one with no nodes in the domain. This solution will yield the lowest possible value of a critical Ra_x, hence attention is focused on this solution only. Solutions for $\phi(y)$ of the form $\phi(y) \propto \exp(\pm \eta y)$ are sought and the procedure follows that of ref. [8] except that Ra there must be replaced by Ra_x here. The six roots for η are thus found and the boundary conditions are applied to the even solutions to find the pertinent constants. The requirement that boundary conditions be satisfied in the case of non-trivial solutions yields, after some straightforward algebra, the condition that:

$$\mathcal{I}\left\{(3+i\sqrt{3})\, Z \tanh\frac{mZx}{2}\right\}+\sqrt{3}\, c \tan\frac{mcx}{2}=0, \tag{24}$$

where $\mathcal{I}$ denotes the imaginary part of the complex number in brackets,

$$Z=\frac{\sqrt{2}}{2}\left\{\left[(1+q+q^2)^{1/2}+\left(1+\frac{q}{2}\right)\right]^{1/2} + i\left[(1+q+q^2)^{1/2}-\left(1+\frac{q}{2}\right)\right]^{1/2}\right\},$$

and

$$c=(q-1)^{1/2},$$

where q here is defined such that:

$$Ra_x = m^4 q^3. \tag{25}$$

Alternatively, at each x, $Ra_H = m^4 q^3 x$ and it is obtained after solving the transcendental equation (24) relating m, x and q. The values of q satisfying equation (24) for each m and x are found numerically using a NAG Fortran Library Routine (COAJF) which locates the zeros of a continuous function by a continuation method using a secant iteration, and the minimum of the characteristic values of Ra_H at each x is then easily found.

Results obtained by this procedure are summarized in Table 1 and Figs. 2 and 3. Table 1 shows the values of m_{crit} and Ra_{crit} at some values of x while in Fig. 2 the variation of Ra_{crit} with location x and the variation of m_{crit} with x are depicted. Figure 3 shows typical curves of the Rayleigh numbers at which instability sets in for disturbances of different wave numbers m, at the different locations x indicated by the number on each curve, for the first even mode. The results are simple and as anticipated. For example, when $x = 1$, the classical solution for the case of two horizontal parallel planes, separated in the vertical by a distance of unity, is obtained; i.e. the critical Rayleigh number

Table 1. The critical values of the Rayleigh number and wave number for various locations along the wedge

x	m_{crit}	Ra_{crit}
0	∞	∞
0.125	24.93	874 374.03
0.250	12.47	109 296.80
0.500	6.23	13 662.10
0.750	4.16	4048.04
1.000	3.12	1707.77
1.500	2.08	506.01
2.000	1.56	213.47
3.000	1.04	63.25
4.000	0.78	26.68
5.000	0.62	13.66
∞	0	0

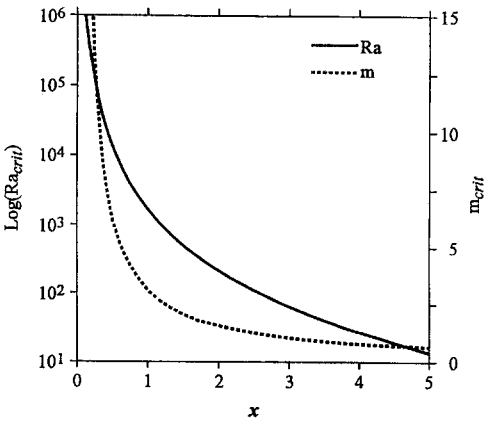

Fig. 2. The lower bound for Ra_{crit} as a function of x (———), and the variation of m_{crit} with x (– – – –).

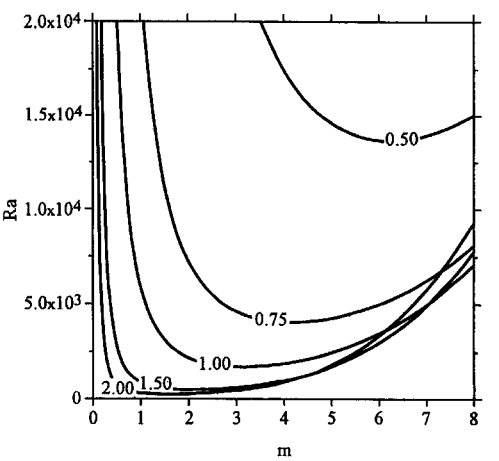

Fig. 3. The Rayleigh numbers at which instabilities set in for perturbations of different wave numbers m for the first mode, at the different positions x indicated by the number on each curve.

at which instability occurs is $Ra_{crit} \approx 1707.765$, for disturbances with $m \approx 3.12$ ($\equiv m_{crit}$).

The curves are all similar as Ra_{crit} decreases with increasing x. Near the tip of the wedge the Rayleigh number necessary for instability is, as expected, much larger than that needed when the boundaries are separated by a larger distance while kept at the same temperature, indicating the removal of the stabilizing influence of boundaries on the flow. In fact, the region very near the tip of a shallow wedge will be always stable since it reaches an average temperature between that of the two adjacent boundaries. The decrease in Ra_{crit} is, however, much slower for values of $x > 1$ than for those values of $x < 1$. Longwave disturbances become unstable at lower values of Ra as x increases for the range $Ra < Ra_{crit}$ while shortwave disturbances become unstable at lower values of Ra for the range $Ra > Ra_{crit}$ only if $x < 1$. For values of $x > 1$ and in the range $Ra > Ra_{crit}$, longwave disturbances need higher values of Ra to go unstable. The crossing over in these curves indicates that when $x > 1$, according to the linear theory, disturbances of the shortwave type will become unstable at values of Ra lower than those corresponding to their local $Ra(m)$ curve obtained by solving equation (24) for large x.

4. SUMMARY

The stability of a known, steady-state, two-dimensional asymptotic solution to secondary flow disturbances was analysed using linear theory. The linear stability analysis provided a lower bound to the critical Ra and predicts that in the limit $A \to 0$ the single-cell circulation is not stable when the global Ra, that defined using the maximum vertical height H that separates the two boundaries at L, increases beyond about 1.8×10^3 for a wedge-like geometry that extends horizontally up to $x = L$. Numerically, ref. [3] found that in triangular enclosures of small aspect ratios the single-cell circulation breaks down into a multicellular pattern when the global Ra is increased beyond the value of about 3×10^3. The linear stability theory yielded a $Ra_{crit} \approx 1707.8$ while numerically the bifurcation occurred at $Ra_{crit} \approx 2886$, about 1.5 times larger than the predicted value.

In ref. [3] the stability of the solutions obtained by ref. [1] to changes in Ra was numerically studied in detail for the case that corresponds to $x = 1$ in the present nomenclature. For the present note some numerical simulations using the model described in ref. [3] were carried out to test the general predictions of the linear stability analysis. The numerical model was adapted to solve the same problem for the cases when the horizontal extent of the cavity is smaller and larger than L, corresponding to the non-dimensional variable $x < 1$ and $x > 1$ used in the stability analysis. Using fixed values of $A = 0.2$ and $Pr = 0.72$, cavities equivalent to $x = 0.5$ and $x = 2$ were considered, and solutions were numerically found for values of Ra varying between 7200 and 72 000 in the first case, and between 72 and 720 in the second. The flow fields developed in the same way as for the experiments with $x = 1$ and it was determined that with $x = 0.5$ numerically $Ra_{crit} \approx 2 \times 10^4$ while, with $x = 2$, $Ra_{crit} \approx 360$. When these values are compared with the theoretical values of Ra_{crit} of Table 1, again the numerical values of Ra_{crit} appear to be about 1.5 times the theoretical ones.

From the experimental measurements described in ref. [9], it was concluded that the onset of convection in a three-dimensional trapezoidal enclosure occurs at progressibly lower Ra as the angle of inclination of the top wall with respect to the horizontal increased from zero. The angle was varied by rotating the upper wall about the horizontal wall, with a fixed point located at the top of the mean cavity height so that the angle of 0° corresponded to a rectangular geometry while the largest angle they achieved converted the (x, y) section of that geometry into a triangular one, with the mean height of the enclosure remaining fixed. Since their definition of Ra was based on the latter, the procedure of varying the angle that way may be thought of as analogous to increasing the location of the 'end' of an originally two-dimensional wedge-like geometry, namely increasing x beyond 1 (or L in dimensional terms) in the present notation, and it is encouraging that in their experiments this results in the same qualitative lowering of the value of Ra_{crit}.

Results from the linear theory are not able to provide an exact Ra_{crit} but they provide a lower bound for Ra_{crit} below which secondary motion of the type assumed in this note will not occur, which is a function of location along the wedge. In the context of the problem at hand, that of a finite triangular cavity, these simple results may be viewed as a guide for the values of Ra that can be allowed for a given geometry once the boundary conditions are specified and if instabilities in the flow are to be prevented.

Acknowledgements—Bram Hauer and Jeff Blundell helped with programming and graphics. I wish to thank Mike Davey, Juan Rivero and Robb McDonald for discussions and comments on the manuscript.

REFERENCES

1. D. Poulikakos and A. Bejan, The fluid mechanics of an attic space, *J. Fluid Mech.* **131**, 251–269 (1983).
2. D. E. Cormack, L. G. Leal and J. Imberger, Natural convection in a shallow cavity with differentially heated end walls. Part 1. Asymptotic theory, *J. Fluid Mech.* **65**, 209–230 (1974).
3. H. Salmun, Convection patterns in a triangular domain, *Int. J. Heat Mass Transfer* **38**, 351–362 (1995).
4. E. M. Sparrow and R. B. Husar, Longitudinal vortices in natural convection flow on inclined surfaces, *J. Fluid Mech.* **37**, 251–255 (1969).
5. J. R. Lloyd and E. M. Sparrow, On the stability of natural convection flow on inclined plates, *J. Fluid Mech.* **42**, 465–470 (1970).
6. J. N. Shadid and R. J. Goldstein, Visualization of longi-

tudinal convection roll instabilites in an inclined enclosure heated from below, *J. Fluid Mech.* **215,** 61–84 (1990).
7. D. E. Farrow and J. C. Patterson, On the stability of the near shore water of a lake when subject to solar heating. *Int. J. Heat Mass Transfer* **36,** 89–100 (1992).
8. S. Chandrasekhar, *Hydrodynamic and Hydromagnetic Stability* (3rd Edn), Chap. II. Oxford University Press, Oxford (1961).
9. S. W. Lam, R. Gani and J. G. Symons, Experimental and numerical studies of natural convection in trapezoidal cavities, *ASME J. Heat Transfer* **111,** 372–377 (1989).